# One-Step Generation of Multifunctional Polyelectrolyte Microcapsules *via* Nanoscale Interfacial Complexation in Emulsion (NICE)

Miju Kim,[†,‡] Seon Ju Yeo,[†,§] Christopher B. Highley,[∥] Jason A. Burdick,[∥] Pil J. Yoo,[§] Junsang Doh,*[,†,‡,⊥] and Daeyeon Lee*[,†]

[†]Department of Chemical and Biomolecular Engineering, University of Pennsylvania, Philadelphia, Pennsylvania 19104, United States, [‡]Department of Mechanical Engineering, Pohang University of Science and Technology (POSTECH), Pohang, Gyeongbuk 790-784, Republic of Korea, [§]School of Chemical Engineering, Sungkyunkwan University (SKKU), Suwon 440-746, Republic of Korea, [∥]Department of Bioengineering, University of Pennsylvania, Philadelphia, Pennsylvania 19104, United States, and [⊥]School of Interdisciplinary Bioscience and Bioengineering (I-Bio), Pohang University of Science and Technology (POSTECH), Pohang, Gyeongbuk 790-784, Republic of Korea

ABSTRACT Polyelectrolyte microcapsules represent versatile stimuli-responsive structures that enable the encapsulation, protection, and release of active agents. Their conventional preparation methods, however, tend to be time-consuming, yield low encapsulation efficiency, and seldom allow for the dual incorporation of hydrophilic and hydrophobic materials, limiting their widespread utilization. In this work, we present a method to fabricate stimuli-responsive polyelectrolyte microcapsules in one step based on nanoscale interfacial complexation in emulsions (NICE) followed by spontaneous droplet hatching. NICE microcapsules can incorporate both hydrophilic and hydro-

phobic materials and also can be induced to trigger the release of encapsulated materials by changes in the solution pH or ionic strength. We also show that NICE microcapsules can be functionalized with nanomaterials to exhibit useful functionality, such as response to a magnetic field and disassembly in response to light. NICE represents a potentially transformative method to prepare multifunctional nanoengineered polyelectrolyte microcapsules for various applications such as drug delivery and cell mimicry.
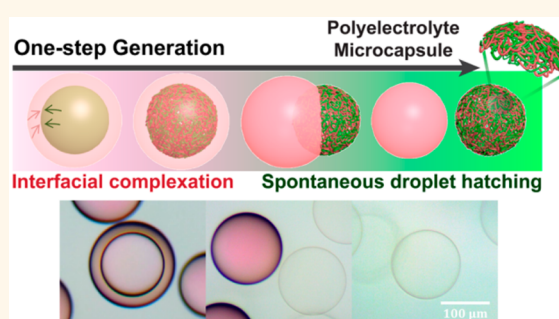
KEYWORDS: polyelectrolyte microcapsule · polyelectrolyte complexes · stimuli-responsive materials · triggered release

Microcapsules encapsulate and protect cargo by forming isolated compartments inside hollow shells. Microcapsules formed from "smart" polymers such as polyelectrolytes enable the triggered release of encapsulated actives in the presence of stimuli such as pH and light, making them useful in the food, pharmaceutical, cosmetics and agricultural applications.[1−14] In addition, polyelectrolyte microcapsules with aqueous cores in an aqueous environment represent a class of "protocells" that enable the recapitulation of cellular functions such as enzyme reactions, gene/protein expression and intercapsule communications.[15−18] These polyelectrolyte microcapsules can be prepared by inducing complexation of two oppositely charged polyelectrolytes, such as through layer-by-layer (LbL) assembly, to form nanoengineered shells that are sensitive to external stimuli. Although polyelectrolyte microcapsules show significant potential for the encapsulation and triggered release of active agents and the mimicry of the living cell,[19−21] their widespread utilization has been hampered by multistep, time-consuming preparation and low encapsulation efficiency. Also, the functionalization of these polyelectrolyte microcapsules with nonwater-soluble materials such as hydrophobic molecules and
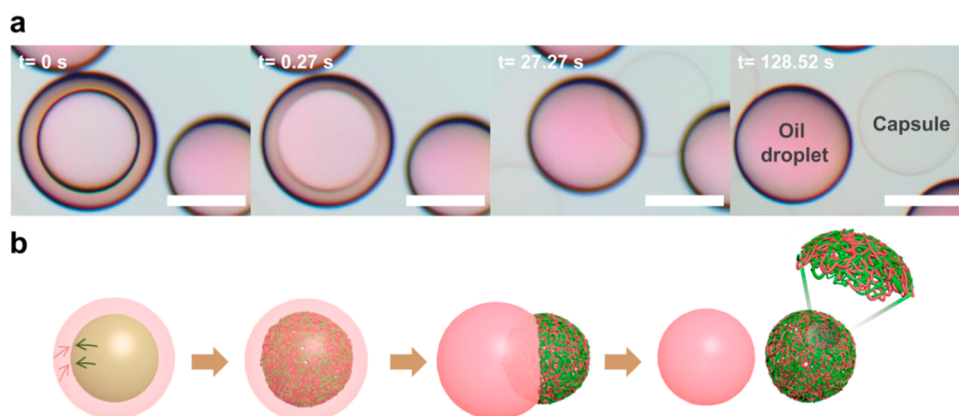
Figure 1. (a) Optical microscopy images showing the generation of (PAA/bPEI) NICE microcapsules through complete droplet hatching. Oil phase (pink) contains 0.001 wt % Nile Red. Scale bar = 100 μm. (b) Schematic illustration describing the NICE process.

nanomaterials is not straightforward. While progress toward overcoming these challenges have been made,[22,23] few methods allow for the one-step generation of multifunctional polyelectrolyte microcapsules with stimuli-responsive properties, high uniformity in dimensions, high encapsulation of actives, and incorporation of functional apolar nanomaterials.[24,25]

In this work, we report a new class of multifunctional polyelectrolyte microcapsules that can be prepared by a one-step process called nanoscale interfacial complexation in emulsion (NICE). The NICE method extends the utility of polyelectrolyte microcapsules and overcomes the major challenges that are presented by conventional polyelectrolyte microcapsule preparation techniques by allowing for one-step microcapsule formation, high encapsulation efficiency and dual incorporation of hydrophilic and hydrophobic species. High encapsulation is achieved by the use of microfluidic water-in-oil-in-water (W/O/W) double emulsions.[26] Nanoscale complexation of two polymers at the inner water/oil (W/O) interface of W/O/W double emulsions followed by spontaneous emulsion hatching leads to the formation of multifunctional polyelectrolyte microcapsules. This method is distinctively different from polyelectrolyte coacervation at the interface of simple oil-in-water emulsions, which leads to the formation of polyelectrolyte complex-covered oil droplets.[27−34] The NICE scheme, in contrast, would generate isolated water compartments in an aqueous environment. In addition to hydrophilic agents in the microcapsulate lumen, hydrophobic molecules or nanoparticles can be incorporated into the nanometric polyelectrolyte shell. We also show that these NICE microcapsules can be ruptured to release encapsulated materials in response to external stimuli. These characteristics make NICE microcapsules ideal for applications involving encapsulation and triggered release of agents and potentially cell mimicry.

RESULTS AND DISCUSSION

Generation and Characterization of (PAA/bPEI) NICE Microcapsule. The NICE method involves the complexation of two polymers that form an insoluble nanolayer at the inner W/O interface of a W/O/W double emulsion. The use of a glass capillary microfluidic device (Supporting Information, Scheme S1) for the preparation of W/O/W double emulsions allows for the complete encapsulation of inner aqueous phase as well as the formation of highly monodisperse microcapsules. Our hypothesis is that the complexation between two polymers at the W/O interface, followed by the removal of the solvent from the oil phase of the W/O/W double emulsion would lead to the formation of polyelectrolyte microcapsules. We use poly(acrylic acid) (PAA) and branched poly(ethylenimine) (bPEI) as the two model polymers as they have been extensively used to prepare polyelectrolyte microcapsules *via* LbL assembly.[35] Because the degree of ionization of these two polymers depends strongly on the solution pH, they offer the potential to tune the properties of microcapsules *via* pH control.[35−42]

We use a microfluidic W/O/W emulsion to prepare NICE microcapsules (Supporting Information, Scheme S1b). To aid the stabilization of these double emulsions, we add poly(vinyl alcohol) (PVA) and sorbitan trioleate to the outer aqueous and middle oil phases, respectively. A mixture of chloroform and hexane in a volume ratio of 1:1 is used as the oil phase. Using these combinations, we are able to form stable PAA aqueous core−bPEI oil shell double emulsions. To our surprise, instead of W/O/W double emulsions becoming polyelectrolyte microcapsules *via* the gradual evaporation of the solvents, we observe the inner aqueous cores spontaneously protruding out of the oil droplets (Figure 1 and Supporting Information, Movie S1). Remarkably, the inner aqueous core does not merge with the external water phase during protrusion, indicating the existence of a shell that protects the inner aqueous core. As shown below, this shell comprises ionically

cross-linked nanoscale complexes of PAA and bPEI that form at the W/O interface. Eventually, these snowman-shaped structures become polyelectrolyte microcapsules upon the complete separation of the inner cores from the oil droplets (Supporting Information, Figure S2b). The spontaneous "hatching" process occurs within a few minutes from double emulsion generation (Supporting Information, Movie S1). Eventually, the polyelectrolyte microcapsules can be readily separated from the "mother" oil droplets that float to the top of the solution (Supporting Information, Figure S2c).

We hypothesize that the complete separation of the inner aqueous cores is induced by dewetting of the oil phase on the interfacial complex layer. Analogous behaviors of inner core protrusion from W/O/W double emulsions have been observed when diblock copolymers, random copolymers, and phospholipids were dissolved in the middle phase of W/O/W double emulsions.[43−46] However, a complete separation of the inner core from the oil phase has been seldom observed.[44,47] The interfacial complexation of bPEI and PAA leads to the ionization of functional groups of the two polymers, rendering the complex layer hydrophilic and, more importantly, oleophobic. We believe that this complex layer is highly incompatible with the oil phase and, thus, undergoes complete hatching to minimize its contact with oil. This hypothesis is supported when we directly observe the wetting behavior of a sessile oil drop on the PAA/bPEI interfacial complex layer (Supporting Information, Scheme S2). We observe that an oil drop that remains at a macroscopic planar W/O interface rolls freely on the PAA/bPEI interfacial film, indicating that this interfacial layer is highly oleophobic (Supporting Information, Movie S2). In contrast, in the absence of the interfacial PAA/bPEI layer, an oil drop immediately wets the interface and merges with the oil subphase (Supporting Information, Movie S3).

To understand the molecular driving force for the formation of the PAA/bPEI interfacial complex layer, we analyze the charge state of PAA using Fourier transform-infrared (FT-IR) spectroscopy. The FT-IR spectrum of the interfacial complex formed at the planar W/O interface (Figure 2a) shows that the degree of ionization of PAA in the interfacial film is ∼30%, suggesting a significant extent of electrostatic complexation. Given that the pK_a of PAA in solution is ∼5.5 and that the pH of the inner aqueous phase is 3.7, it is interesting that the degree of PAA ionization in the interfacial complex layer is much greater than that in a pH 3.7 solution. We believe that the amine groups of bPEI in the oil phase become protonated as they encounter the acidic aqueous phase. In addition, the protonation of the amine groups of bPEI can be induced by the deprotonation of carboxylic acid groups of PAA that accumulate at the W/O interface[48] and the subsequent transfer of protons from PAA to bPEI. In turn, the complexation of

oppositely charged functional groups would lead to the formation of the ionically stitched polyelectrolyte complex layer. The ionization of PAA in the interfacial complex layer, despite the low pH condition, is analogous to an increase in the degree of ionization of PAA in the LbL films relative to the solution value at an acidic pH.[49] This shift in the apparent pK_a of PAA has been attributed to the lowered energy barrier for the ionization of PAA in the presence of positively charged functional groups.

To observe how much of PAA participates in the formation of the interfacial complex layer, we use fluorescently labeled PAA to check for residual PAA in the core of NICE microcapsules. Confocal fluorescence microscopy of NICE microcapsule shows that PAA is indeed found in the capsule wall and that little PAA is left in the lumen (Figure 2b), indicating most, if not all, of PAA is incorporated into the complex; however, we cannot completely rule out the existence of a trace amount of free PAA below the detection limit of confocal microscopy. The shell thickness of a NICE microcapsule, determined by atomic force microscopy of dried NICE microcapsules, is 46.4 ± 7.7 nm (Figure 2c−d) and is in good agreement with an estimate based on the total amount of PAA and bPEI present in each double emulsion droplet (see Supporting Information, Equation S1 for details).

The use of W/O/W double emulsions enables the dual incorporation of hydrophilic and hydrophobic agents in NICE microcapsules. When we add fluorescein isothiocyanate (FITC) labeled dextran in the inner aqueous phase and a hydrophobic dye, Nile Red, in the oil phase (Figure 2e), FITC−dextran remains in the aqueous core, and Nile Red is incorporated in the polyelectrolyte complex shell of the NICE microcapsules (Figure 2f). Although the interfacial complex layer is hydrophilic, a small fraction of hydrophobic molecules dissolved in oil phase likely become kinetically trapped in the complex layer during polyelectrolyte complexation. It is also possible that residual sorbitan trioleate in the complex layer aids in the entrapment of the hydrophobic species. This capability to encapsulate hydrophilic and hydrophobic species in the core and the shell of microcapsules, respectively, without any complex procedures offers a significant advantage over conventional polyelectrolyte microcapsules for applications that require the encapsulation and release of species of opposite polarity.[46,50] Also as will be demonstrated below, this capability enables the one-step incorporation of hydrophobic and uncharged nanomaterials in the shell, imparting additional functionality to NICE microcapsules.

Stimuli-Responsive Properties of (PAA/bPEI) NICE Microcapsule. A hallmark of polyelectrolyte microcapsules is their stimuli-responsive properties. Because polyelectrolytes and their complexes can drastically change their internal structures under changes in the pH or
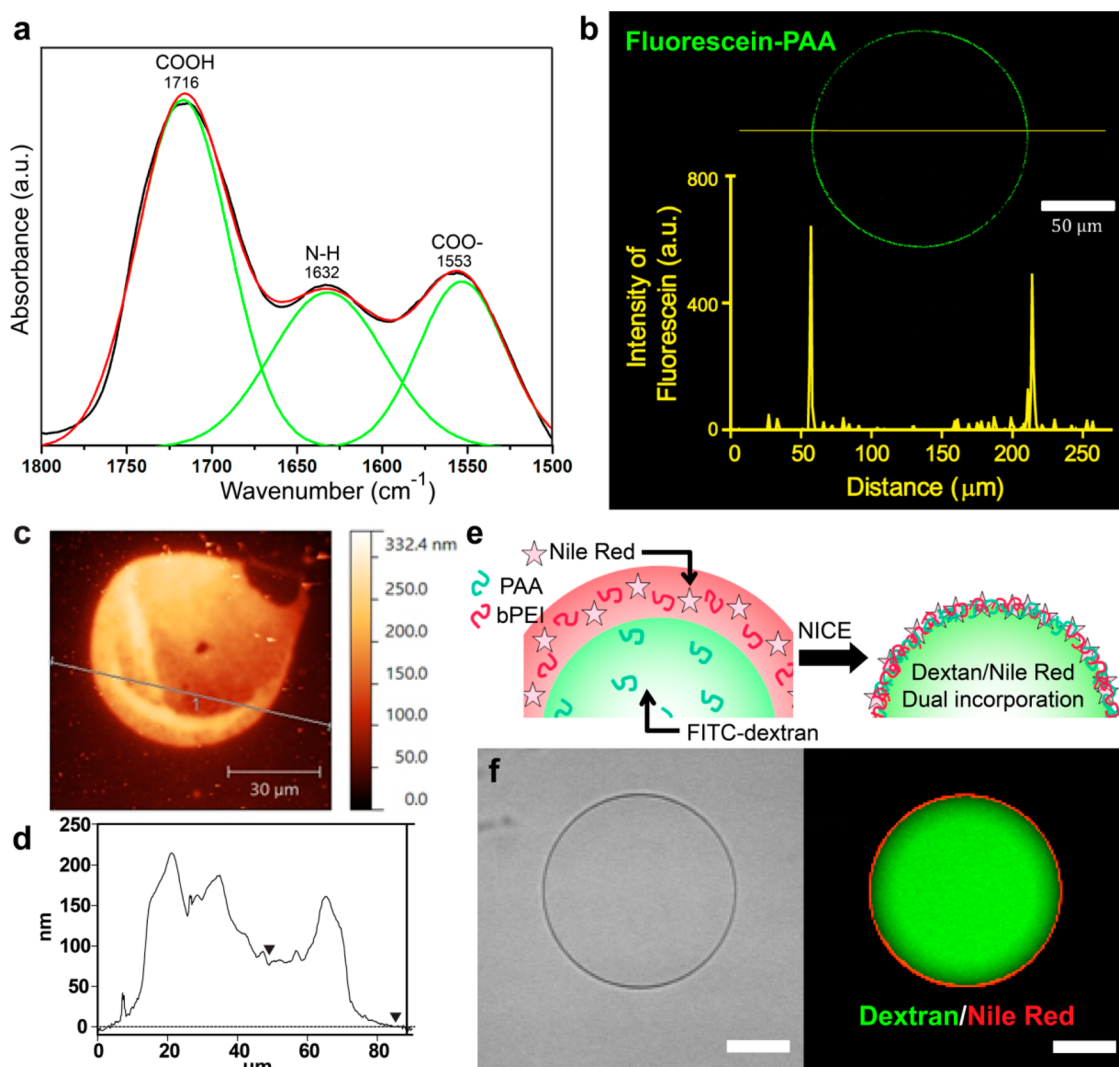
Figure 2. (a) FT-IR spectrum of PAA/bPEI interfacial film. (b) Fluorescence intensity along the yellow straight line drawn on confocal microscopy image of (PAA/bPEI) NICE microcapsule made with fluorescein-labled PAA. (c) AFM height image of (PAA/bPEI) NICE microcapsule. (d) Height profile along the line drawn in panel c. (e) Schematic illustration describing dual incorporation of FITC−dextran and Nile Red. (f) Confocal microscopy images showing an NICE microcapsule incorporating FITC−dextran (green) and Nile Red (red) in the core and shell of the microcapsule, respectively. Scale bar = 50 μm.

ionic strength, polyelectrolyte microcapsules have been shown to exhibit triggered release properties.[37] To demonstrate that NICE microcapsules indeed have such stimuli-responsiveness, we monitor the behaviors of NICE microcapsules under changes in the solution pH or ionic strength. At or below pH 5, these NICE microcapsules keep their shape without any changes (Figure 3a,c). In contrast, at or above pH 7, NICE microcapsules swell significantly until they become invisible under optical microscopy (Figure 3b,e; Supporting Information, Movie S4). Accordingly, the fluorescence intensity owing to the encapsulated FITC−dextran decreases drastically upon the enormous swelling and disassembly of (PAA/bPEI) NICE microcapsules (Figure 3d,f; Supporting Information, Movie S5). The changes in the pH likely induce sudden changes in the interactions between the two polymers leading to drastic swelling. Previous reports using LbL

microcapsules have also shown analogous swelling when the solution pH is shifted toward the pK_a of one of the polyelectrolytes.[51,52]

(PAA/bPEI) NICE microcapsules show triggered release upon changes in the ionic strength of the solution as well. As the ionic strength of the solution is increased by 100-fold from 1 to 100 mM, NICE microcapsules undergo sudden deformation and release the encapsulated FITC−dextran (Figure 4a; Supporting Information, Movie S6). The release rate of inner contents from the NICE microcapsules increases with ionic strength, likely due to the screening of electrostatic attractions between the two polymers and potentially osmotically induced collapse of the shell at upon the addition of salt to the solution (Figure 4b).[8]

Functionalization of NICE Microcapsules *via* Nanomaterial Incorporation. A versatile way to impart functionality to polyelectrolyte microcapsules is the incorporation
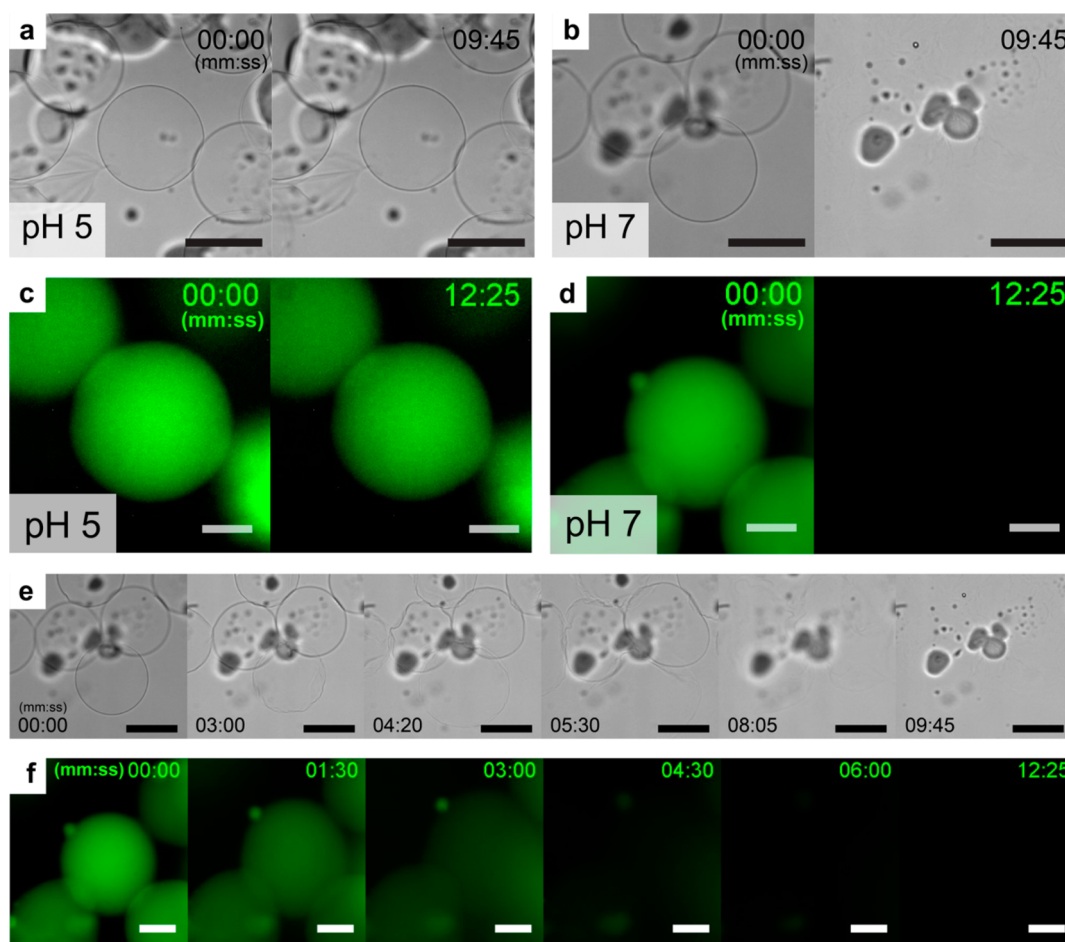
Figure 3. Optical microscopy images of (PAA/bPEI) NICE microcapsules showing pH-triggered responses in (a) pH 5 and (b) pH 7 solutions. Fluorescence microscopy images of (PAA/bPEI) NICE microcapsules containing FITC−dextran (molecular weight: 4000 g/mol) showing pH-triggered release of FITC−dextran at (c) pH 5 and (d) pH 7. (e) Time-lapse images of (b). (f) Time-lapse fluorescence images of (d). Scale bars of (a), (b), (e) = 100 μm. Scale bars of (c), (d), (f) = 50 μm.
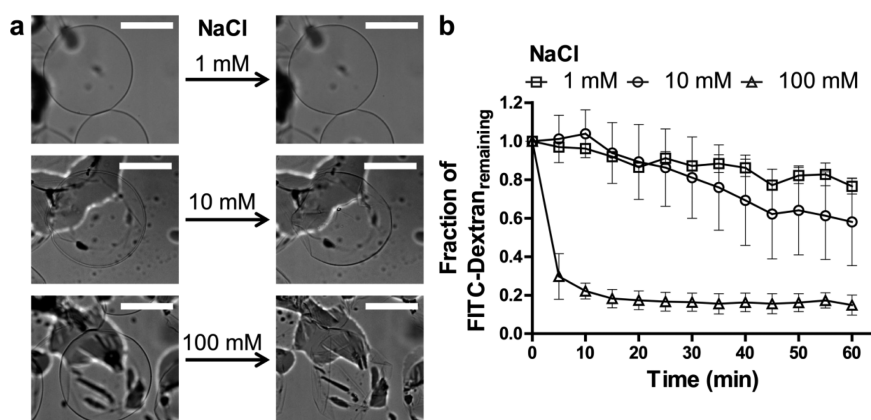

Figure 4. (a) NICE microcapsules showing salt-triggered release; deformations of capsules in (top) 1 mM, (middle) 10 mM, and (bottom) 100 mM NaCl solutions, respectively. Duration = 620 s. (b) Release profiles representing the relative fluorescence intensity (I_t) of 4 kDa FITC−dextran remaining in NICE microcapsules normalized by initial fluorescence intensity (I_0) under different NaCl concentrations. Error bars are standard deviations. All scale bars = 100 μm.

of nanoparticles. Typically, such functionalization is achieved by using charged nanoparticles in LbL assembly, which precludes the incorporation of hydrophobic and/or uncharged nanomaterials. Motivated by the incorporation of a hydrophobic dye, we test the

possibility of incorporating hydrophobic as well as uncharged nanoparticles in the shell by adding hydrophobic magnetic nanoparticles in the NICE microcapsule shell. Such a demonstration would be extremely useful since several functional nanoparticles such as
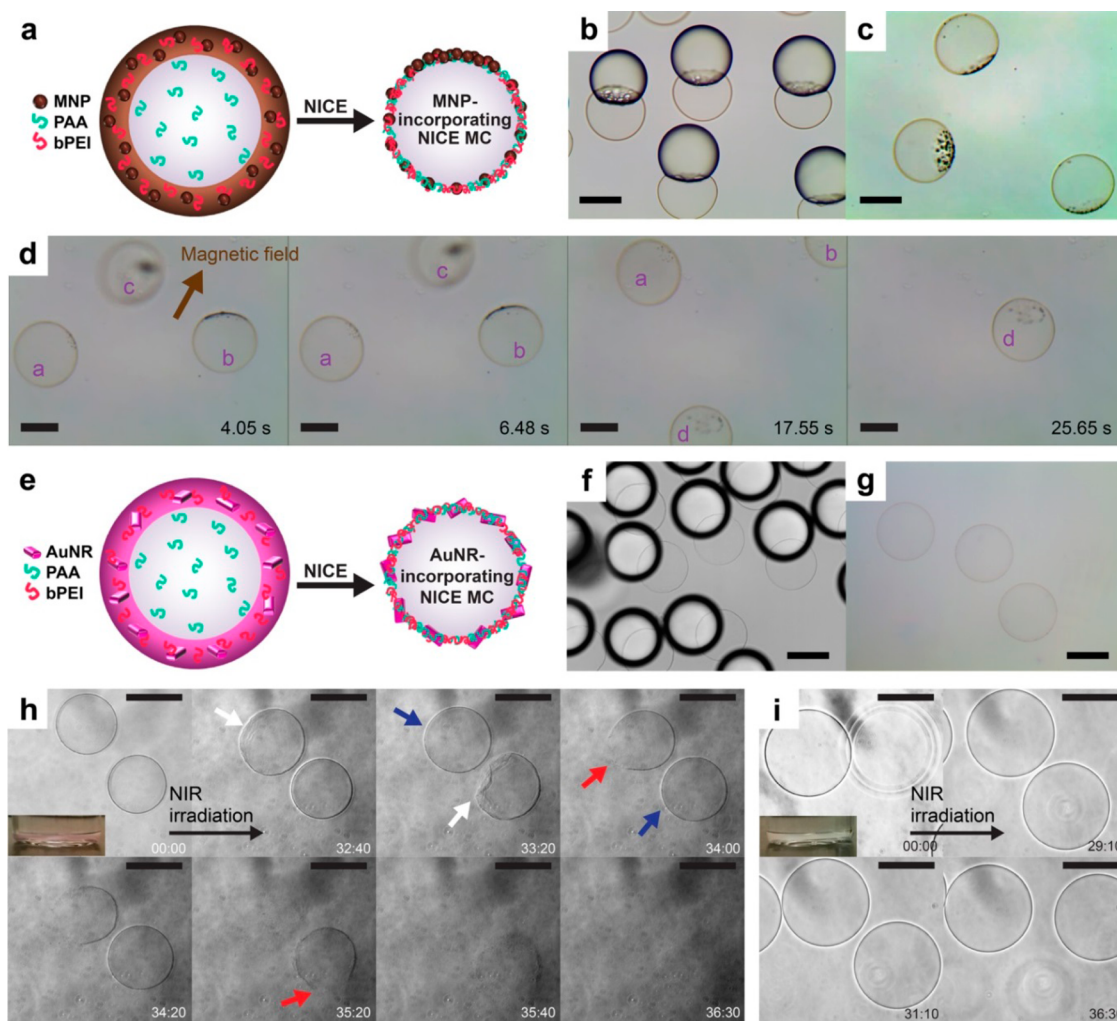
Figure 5. (a) Schematic illustration describing the generation of magnetic nanoparticle (MNP)-incorporating NICE microcapsule (MC). (b) Partial dewetting on the inner aqueous core during the generation of magnetic nanoparticle-incorporating NICE microcapsules. (c) Magnetic nanoparticle-incorporating NICE microcapsules containing a high concentration of magnetic nanoparticles. (d) Time-lapse sequential images showing movements of magnetic nanoparticle-incorporating NICE microcapsules toward a magnetic field gradient. (e) Schematic illustration describing the generation of gold nanorod (AuNR)-incorporating NICE microcapsule. (f) Intermediate dewetting structures with inner cores completely coming out. (g) AuNR-incorporating NICE microcapsules. (h and i) Sequential images showing NIR light-triggered responses of (h) AuNR-incorporating NICE microcapsules (a photo image in $t = 0$ shows violet accumulation of the AuNR-incorporating NICE microcapsules); numbers in the lower right of each image indicate time in minutes and seconds (mm:ss); white, blue, and red arrows show local shrinking, swelling, and catastrophic failure, respectively). (i) NICE microcapsules without AuNRs (a photo image in $t = 0$ shows white accumulation of the plain NICE microcapsules). All of time marks shown in (h) and (i) represent minute:second. All scale bars = 100 μm.

quantum dots and magnetic nanoparticles are synthesized in highly nonpolar organic solvents,[53,54] and such nonwater-soluble nanoparticles cannot be readily incorporated into polyelectrolyte microcapsules, unless nanoparticles with specific ligands are used.[22,23] Hydrophobic magnetic nanoparticles are incorporated into the NICE microcapsule shell by dispersing them in the oil phase of W/O/W double emulsions (Figure 5a). Figure 5c shows that the magnetic nanoparticles dispersed in the oil phase are successfully incorporated in the shell. Interestingly, in the presence of the hydrophobic nanoparticle, we observe partial dewetting (Figure 5b); that is, the oil phase does not completely separate from the protruding NICE microcapsules.

We believe partial dewetting is due to the hydrophobization of PAA/bPEI complex layer in the presence of hydrophobic magnetic nanoparticles and potentially pinning of the contact line during dewetting. Indeed when the concentration of magnetic nanoparticles in the oil phase is increased, the three phase contact angle is decreased, and dewetting is further suppressed (Supporting Information, Figure S3a). Some of magnetic nanoparticles originally present in the oil phase are distributed throughout the shell of NICE microcapsules, likely due to kinetic trapping, as evidenced by the coloration of NICE microcapsules (Figure 5c; Supporting Information, Figure S3b). Also, a small patch of aggregated magnetic nanoparticles is observed in one region

of NICE microcapsules after the complete removal of the solvent. These magnetic nanoparticle-incorporated NICE microcapsules move in the direction of a magnetic field gradient, while pointing their patches toward the direction of the magnetic field gradient (Supporting Information, Movie S7; Figure 5d). These results show that hydrophobic nanoparticles can be directly incorporated into the shell of NICE microcapsules without any tedious ligand exchange processes, significantly simplifying the functionalization of polyelectrolyte microcapsules with functional nanomaterials. The patches of nanoparticles on NICE microcapsules can potentially be used to induce self-propelled motion driven by catalytic reactions.[55]

The functionalization of NICE microcapsules using nanoparticles is further demonstrated by incorporating a plasmonic nanomaterial and testing their light-responsive properties. We incorporate uncharged gold nanorods (AuNRs) in the NICE microcapsule shell by dispersing poly(ethylene glycol)-functionalized AuNRs with bPEI in the oil phase (Figure 5e). AuNR-incorporating NICE microcapsules undergo complete dewetting from the oil phase (Figure 5f,g; Supporting Information, Figure S3c), likely due to the hydrophilic nature of AuNRs. The incorporation of AuNRs in NICE microcapsules is evident by the appearance of violet color from the capsules (Figure 5h inset).

AuNRs are known to generate heat under near-infrared (NIR) irradiation due to their surface plasmon band and thus have been shown to induce NIR-triggered release of molecules from various structures.[46,56−60] NIR is an especially attractive stimulus because of its ability to penetrate tissue with minimal absorption and ease of localized stimulus application. AuNR-incorporating NICE microcapsules indeed undergo catastrophic rupture under NIR irradiation (1 W output power at 808 nm for approximately 40 min; Figure 5h; Supporting Information, Movie S8). These microcapsules undergo significant volumetric fluctuations such as shrinking (white arrows in Figure 5h) and swelling (blue arrows in Figure 5h) before catastrophic failure occurs in one region (red arrows in Figure 5h).

Under the same irradiation condition, neat NICE microcapsules undergo neither volumetric fluctuations nor catastrophic rupture (Figure 5i).

CONCLUSIONS

In this work, we have presented the one-step generation of multistimuli-responsive polyelectrolyte microcapsules with high encapsulation and dual incorporation of both hydrophilic and hydrophobic species using nanoscale interfacial complexation in emulsion (NICE). The novelty of this method lies in the interfacial complexation of two polyelectrolytes at the inner interface of W/O/W double emulsions and the complete hatching of the inner droplets from the oil phase of W/O/W double emulsions, leading to the formation of highly uniform and multifunctional NICE microcapsules. NICE microcapsules undergo triggered release of the encapsulants in response to changes in the pH and ionic strength of solutions. NICE also enables the incorporation of hydrophobic/uncharged molecules and nanomaterials in the nanoshell, drastically expanding the palette of materials that can be used to functionalize polyelectrolyte microcapsules. This new approach overcomes some of the major challenges that are associated with conventional polyelectrolyte microcapsule generation techniques and suggests an entirely new one-step method to generate highly functional polyelectrolyte microcapsules that should be widely applicable. By varying the fabrication conditions such as sets of polyelectrolytes, pH and ionic strengths, NICE microcapsules with a broad range of functionalities can be generated. This method also should be highly scalable by the parallelization of the double emulsion formation process[61−63] and could be extended to produce submicrometer NICE microcapsules by using a previously reported osmotic annealing method,[64] making it a potentially transformative method of polyelectrolyte microcapsule preparation. Our current efforts include enabling the formation of NICE microcapsules based on biopolymers such as proteins and polysaccharides, which typically have low solubility in organic solvents.

METHODS

Generation of NICE Microcapsules. We use a previously reported glass-capillary microfluidic device for the preparation of water-in-oil-in-water (W/O/W) double emulsions.[46] To generate monodisperse W/O/W double emulsions, we used 0.1 wt % of PAA dissolved in deionized water (pH 3.7) as the inner phase, 0.1 wt % bPEI dissolved in a mixture of chloroform and hexane (Fisher Scientific) in a volume ratio of 1:1 containing 1−2 wt % sorbitan trioleate as the middle phase, and 2 wt % poly(vinyl alcohol) (PVA, 87−90% hydrolyzed, average molecular weight: 30 000−70 000 g/mol, Sigma-Aldrich) solution as the outer phase. These three flows were introduced and controlled by using three syringe pumps. Generated double emulsions were collected in pH 2-adjusted water. To test the stability of double emulsions and observe dewetting phenomena, we varied the

collection medium to pure deionized water and pH 3 and pH 9 water. We find that the condition of the continuous phase plays a critical role in maintaining the structural integrity of NICE microcapsules during inner core protrusion from double emulsions. When the continuous aqueous phase is deionized water (pH 5.5−6), we observe that the volume of the inner droplets shrinks gradually during protrusion. In contrast, when we collect double emulsions in acidic water (pH 2), the protruded inner droplets remain stable without any shrinkage during protrusion and subsequent separation (Supporting Information, Figure S2a). These observations strongly suggest that the polyelectrolyte complex layer is experiencing some type of tension under pH 5.5−6 and that this tension drives the capsule shrinkage. The relative magnitudes of shell elasticity and membrane tension likely determine whether microcapsules form

without any significant volume changes during dewetting. The origin of the membrane tension, as well as the effect of the solution pH on the membrane tension and the stability of NICE microcapsules, warrants future study.

Synthesis of Fluorescein Labeled PAA. PAA (M_w: 345 000 g/mol, 200 mg) was dissolved in 20 mL of deionized water, and the solution pH was adjusted to 5.0. Final molar concentration of carboxylic acid groups of the solution was 0.138 M, and 1 mol % of the carboxylic acid groups (1.38 mM) was targeted for this conjugation. Carboxylic acid groups of PAA were activated using 1-ethyl-3-(3-(dimethylamino)propyl)carbodiimide (EDC, Sigma-Aldrich) and N-hydroxysuccinimide (NHS, Sigma-Aldrich). A total of 21.16 mg of EDC (5.5 mM) and 12.71 mg of NHS (5.5 mM) were added to the PAA solution in a molar ratio of 4:4:1 (EDC/NHS/AA) and the mixture was stirred for 1 h at room temperature. Then, 9.59 mg of 6-aminofluorescein (1.38 mM, Sigma-Aldrich) was added and the mixture was stirred for 12 h at room temperature. The reacted solution was dialyzed for 48 h to remove unreacted 6-aminofluorescein using a 10K MWCO dialysis cassette The fluorescein labeled PAA solution was stored at 4 °C. When we used the fluorescein–PAA as the inner phase, we diluted the solution three times by mixing with 0.1 wt % unlabeled PAA.

Atomic Force Microscopy (AFM). The dried NICE microcapsules were prepared on cleaned silicon wafers. Size of the NICE microcapsules suspended in aqueous solution was about 130 μm. The thickness measurements were performed using Dimension Icon Atomic Force Microscope (Bruker, Inc.) at 25.0 ± 0.5 °C. Silicon cantilevers with a resonance frequency about 380 kHz were utilized for tapping mode at a scan rate of 1.02 Hz.

Dual Incorporation of Nile Red and FITC–Dextran. To examine the dual incorporation of both FITC–dexran (Sigma-Aldrich, average molecular weight: 4000 g/mol) and Nile Red (Sigma-Aldrich), we added 0.2 wt % FITC–dextran and 0.01 wt % Nile Red to the inner aqueous phase and middle phase solutions, respectively. We used 0.2 wt % FITC–dextran as inner contents for testing the triggered release as well.

Generation of Magnetic Nanoparticle-Incorporating NICE Microcapsule. First, we prepared chloroform-dispersed magnetic nanoparticles. The initial product (Magnetic nanoparticles, Ferrofluid, FerroTec) was dispersed in toluene. To disperse magnetic nanoparticles in the oil phase, we exchanged the original solvent to chloroform by evaporating the solvent and redispersing magnetic nanoparticles in chloroform with sonication. This process provided a uniform brown solution containing well-dispersed magnetic nanoparticles. We made a mixture consisting of chloroform (50 v/v%), hexane (50 v/v%), sorbitan trioleate (1 wt %), and magnetic nanopaticles (0.05 wt %) and generated double emulsions. Double emulsion collection was made in pH 2-adjusted water. Centrifugation was used to remove residual oil droplets upon partial dewetting.

Generation of AuNR-Incorporating NICE Microcapsule. All materials for gold nanorods (AuNRs) synthesis were purchased from Sigma-Aldrich. AuNRs were synthesized by an established seed-growth method.[56] Briefly, a solution of gold(III) chloride trihydrate, hexadecyltrimethylammonium bromide (CTAB), and sodium borohydride established Au seed nanoparticles, which were then added to a solution of gold(III) chloride trihydrate, CTAB, silver nitrate, and ascorbic acid to induce Au nanorod growth. AuNR formation was confirmed by UV–vis spectroscopy, which showed the characteristic transverse and longitudinal absorbance peaks for the gold nanorods (at approximately 515 and 800 nm, respectively). The nanorods were then washed by centrifugation and resuspended in an aqueous solution of poly(ethylene glycol)-thiol (MW = 5 kDa) for PEGylation. After PEGylation, we centrifuged the NPs and resuspended them in chloroform. The final concentration of nanorods in chloroform was determined by measuring peak absorbance of the suspension and applying the Beer–Lambert law with a molar extinction coefficient of 4.4×10^9 M^{-1} cm^{-1}.

With the chloroform-dispersed AuNRs, we made an oil phase solution consisting of chloroform (50 v/v%), hexane (50 v/v%), sorbitan trioleate (1 wt %), and AuNRs (0.8 nM), with which we generated double emulsions. Double emulsion collection was made in pH 2-adjusted water. After collection of

NICE microcapsules, we exchanged the supernatant to pH 2-adjusted water several times to remove residual solvent. For near-infrared irradiation, we used a NIR laser (OEM Laser Systems). The prepared NICE microcapsules with/without AuNRs were placed on a microscope stage and exposed to NIR laser with 1 W output power at 808 nm. We performed live imaging using inverted microscope (Carl Zeiss).

Optical Imaging. For fluorescence imaging, we used a confocal laser scanning microscope (Olympus FluoView FV1000, Center Valley, PA) or a epi-fluorescence inverted microscope (Nikon Diaphot 300) with a CCD camera (Qimaging Retiga 2000R Fast 1394). Bright field imaging was also performed with a Nikon Diaphot 300 microscope. For colored digital imaging, we used an upright microscope (Carl Zeiss Axio Plan II) with a digital camera (AmScope MU1003-CK 10MP). All of images were analyzed with ImageJ (NIH).

Conflict of Interest: The authors declare no competing financial interest.

Supporting Information Available: Schematic illustrations showing experimental details, analysis of a macroscopic PAA/bPEI interfacial film at a planar oil–water interface, entire PAA/bPEI FT-IR spectrum, effect of pH conditions on the formation of NICE microcapsules, shell thickness estimation, images showing various dewetting structures of magnetic nanoparticle-incorporating double emulsions, coloration images of magnetic nanoparticle or AuNR-incorporating NICE microcapsules and descriptions of all movies (Movies S1–S8). The Supporting Information is available free of charge on the ACS Publications website at DOI: 10.1021/acsnano.5b02702.

REFERENCES AND NOTES

1. Zhang, J.; Coulston, R. J.; Jones, S. T.; Geng, J.; Scherman, O. A.; Abell, C. One-Step Fabrication of Supramolecular Microcapsules from Microfluidic Droplets. *Science* **2012**, *335*, 690–694.

2. Chang, T. M. Semipermeable Microcapsules. *Science* **1964**, *146*, 524–525.

3. Ejima, H.; Richardson, J. J.; Liang, K.; Best, J. P.; van Koeverden, M. P.; Such, G. K.; Cui, J.; Caruso, F. One-Step Assembly of Coordination Complexes for Versatile Film and Particle Engineering. *Science* **2013**, *341*, 154–157.

4. De Koker, S.; De Cock, L. J.; Rivera-Gil, P.; Parak, W. J.; Auzély Velty, R.; Vervaet, C.; Remon, J. P.; Grooten, J.; De Geest, B. G. Polymeric Multilayer Capsules Delivering Biotherapeutics. *Adv. Drug Delivery Rev.* **2011**, *63*, 748–761.

5. Peyratout, C. S.; Dähne, L. Tailor-Made Polyelectrolyte Microcapsules: From Multilayers to Smart Containers. *Angew. Chem., Int. Ed.* **2004**, *43*, 3762–3783.

6. Esser-Kahn, A. P.; Odom, S. A.; Sottos, N. R.; White, S. R.; Moore, J. S. Triggered Release from Polymer Capsules. *Macromolecules* **2011**, *44*, 5539–5553.

7. Wang, H.-C.; Zhang, Y.; Possanza, C. M.; Zimmerman, S. C.; Cheng, J.; Moore, J. S.; Harris, K.; Katz, J. S. Trigger Chemistries for Better Industrial Formulations. *ACS Appl. Mater. Interfaces* **2015**, *7*, 6369–6382.

8. Gao, C.; Leporatti, S.; Moya, S.; Donath, E.; Möhwald, H. Swelling and Shrinking of Polyelectrolyte Microcapsules in

Response to Changes in Temperature and Ionic Strength. *Chem. - Eur. J.* **2003**, *9*, 915–920.

9. Levy, T.; Dejugnat, C.; Sukhorukov, G. B. Polymer Microcapsules with Carbohydrate-Sensitive Properties. *Adv. Funct. Mater.* **2008**, *18*, 1586–1594.

10. Stoychev, G.; Puretskiy, N.; Ionov, L. Self-Folding All-Polymer Thermoresponsive Microcapsules. *Soft Matter* **2011**, *7*, 3277–3279.

11. Bird, R.; Freemont, T.; Saunders, B. R. Tuning the Properties of pH-Responsive and Redox Sensitive Hollow Particles and Gels Using Copolymer Composition. *Soft Matter* **2012**, *8*, 1047–1057.

12. Yi, Q.; Sukhorukov, G. B. Externally Triggered Dual Function of Complex Microcapsules. *ACS Nano* **2013**, *7*, 8693–8705.

13. Liang, K.; Such, G. K.; Johnston, A. P.; Zhu, Z.; Ejima, H.; Richardson, J. J.; Cui, J.; Caruso, F. Endocytic pH-Triggered Degradation of Nanoengineered Multilayer Capsules. *Adv. Mater.* **2014**, *26*, 1901–1905.

14. Ammala, A. Biodegradable Polymers as Encapsulation Materials for Cosmetics and Personal Care Markets. *Int. J. Cosmet. Sci.* **2013**, *35*, 113–124.

15. Tiourina, O.; Radtchenko, I.; Sukhorukov, G.; Möhwald, H. Artificial Cell Based on Lipid Hollow Polyelectrolyte Microcapsules: Channel Reconstruction and Membrane Potential Measurement. *J. Membr. Biol.* **2002**, *190*, 9–16.

16. Kolmakov, G. V.; Yashin, V. V.; Levitan, S. P.; Balazs, A. C. Designing Communicating Colonies of Biomimetic Microcapsules. *Proc. Natl. Acad. Sci. U. S. A.* **2010**, *107*, 12417–12422.

17. Kamat, N. P.; Katz, J. S.; Hammer, D. A. Engineering Polymersome Protocells. *J. Phys. Chem. Lett.* **2011**, *2*, 1612–1623.

18. Martino, C.; Kim, S. H.; Horsfall, L.; Abbaspourrad, A.; Rosser, S. J.; Cooper, J.; Weitz, D. A. Protein Expression, Aggregation, and Triggered Release from Polymersomes as Artificial Cell-Like Structures. *Angew. Chem., Int. Ed.* **2012**, *51*, 6416–6420.

19. Caruso, F.; Caruso, R. A.; Möhwald, H. Nanoengineering of Inorganic and Hybrid Hollow Spheres by Colloidal Templating. *Science* **1998**, *282*, 1111–1114.

20. De Geest, B. G.; Sanders, N. N.; Sukhorukov, G. B.; Demeester, J.; De Smedt, S. C. Release Mechanisms for Polyelectrolyte Capsules. *Chem. Soc. Rev.* **2007**, *36*, 636–649.

21. Delcea, M.; Möhwald, H.; Skirtach, A. G. Stimuli-Responsive LbL Capsules and Nanoshells for Drug Delivery. *Adv. Drug Delivery Rev.* **2011**, *63*, 730–747.

22. Lee, B.; Kim, Y.; Lee, S.; Kim, Y. S.; Wang, D.; Cho, J. Layer-by-Layer Growth of Polymer/Quantum Dot Composite Multilayers by Nucleophilic Substitution in Organic Media. *Angew. Chem., Int. Ed.* **2010**, *49*, 359–363.

23. Tettey, K. E.; Yee, M. Q.; Lee, D. Layer-by-Layer Assembly of Charged Particles in Nonpolar Media. *Langmuir* **2010**, *26*, 9974–9980.

24. Kaufman, G.; Boltyanskiy, R.; Nejati, S.; Thiam, A. R.; Loewenberg, M.; Dufresne, E. R.; Osuji, C. O. Single-Step Microfluidic Fabrication of Soft Monodisperse Polyelectrolyte Microcapsules by Interfacial Complexation. *Lab Chip* **2014**, *14*, 3494–3497.

25. Wang, Q.; Schlenoff, J. B. Single-and Multicompartment Hollow Polyelectrolyte Complex Microcapsules by One-Step Spraying. *Adv. Mater.* **2015**, *27*, 2077–2082.

26. Utada, A.; Lorenceau, E.; Link, D.; Kaplan, P.; Stone, H.; Weitz, D. Monodisperse Double Emulsions Generated from a Microcapillary Device. *Science* **2005**, *308*, 537–541.

27. Dickinson, E. Interfacial Structure and Stability of Food Emulsions as Affected by Protein−Polysaccharide Interactions. *Soft Matter* **2008**, *4*, 932–942.

28. Dardelle, G.; Erni, P. Three-Phase Interactions and Interfacial Transport Phenomena in Coacervate/Oil/Water Systems. *Adv. Colloid Interface Sci.* **2014**, *206*, 79–91.

29. Li, J.; Hughes, A. D.; Kalantar, T. H.; Drake, I. J.; Tucker, C. J.; Moore, J. S. Pickering-Emulsion-Templated Encapsulation of a Hydrophilic Amine and Its Enhanced Stability Using Poly (Allyl Amine). *ACS Macro Lett.* **2014**, *3*, 976–980.

30. Zheng, Y.; Yu, Z.; Parker, R. M.; Wu, Y.; Abell, C.; Scherman, O. A. Interfacial Assembly of Dendritic Microcapsules with Host−Guest Chemistry. *Nat. Commun.* **2014**, *5*, 5772.

31. Le Tirilly, S.; Tregouët, C.; Bône, S. P.; Geffroy, C. D.; Fuller, G.; Pantoustier, N. G.; Perrin, P.; Monteux, C. C. Interplay of Hydrogen Bonding and Hydrophobic Interactions to Control the Mechanical Properties of Polymer Multilayers at the Oil−Water Interface. *ACS Macro Lett.* **2015**, *4*, 25–29.

32. Kizilay, E.; Kayitmazer, A. B.; Dubin, P. L. Complexation and Coacervation of Polyelectrolytes with Oppositely Charged Colloids. *Adv. Colloid Interface Sci.* **2011**, *167*, 24–37.

33. Monteillet, H.; Hagemans, F.; Sprakel, J. Charge-Driven Co-Assembly of Polyelectrolytes across Oil−Water Interfaces. *Soft Matter* **2013**, *9*, 11270–11275.

34. de Silva, U. K.; Weik, B. E.; Lapitsky, Y. Simple Preparation of Polyelectrolyte Complex Beads for the Long-Term Release of Small Molecules. *Langmuir* **2014**, *30*, 8915–8922.

35. Tong, W.; Gao, C.; Möhwald, H. Stable Weak Polyelectrolyte Microcapsules with pH-Responsive Permeability. *Macromolecules* **2006**, *39*, 335–340.

36. Shiratori, S. S.; Rubner, M. F. pH-Dependent Thickness Behavior of Sequentially Adsorbed Layers of Weak Polyelectrolytes. *Macromolecules* **2000**, *33*, 4213–4219.

37. Tong, W.; Song, X.; Gao, C. Layer-by-Layer Assembly of Microcapsules and Their Biomedical Applications. *Chem. Soc. Rev.* **2012**, *41*, 6103–6124.

38. Antipov, A. A.; Sukhorukov, G. B.; Leporatti, S.; Radtchenko, I. L.; Donath, E.; Möhwald, H. Polyelectrolyte Multilayer Capsule Permeability Control. *Colloids Surf., A* **2002**, *198-200*, 535–541.

39. Chung, A.; Rubner, M. Methods of Loading and Releasing Low Molecular Weight Cationic Molecules in Weak Polyelectrolyte Multilayer Films. *Langmuir* **2002**, *18*, 1176–1183.

40. Mendelsohn, J. D.; Yang, S. Y.; Hiller, J. A.; Hochbaum, A. I.; Rubner, M. F. Rational Design of Cytophilic and Cytophobic Polyelectrolyte Multilayer Thin Films. *Biomacromolecules* **2003**, *4*, 96–106.

41. Mauser, T.; Déjugnat, C.; Sukhorukov, G. B. Balance of Hydrophobic and Electrostatic Forces in the pH Response of Weak Polyelectrolyte Capsules. *J. Phys. Chem. B* **2006**, *110*, 20246–20253.

42. Usov, D.; Sukhorukov, G. B. Dextran Coatings for Aggregation Control of Layer-by-Layer Assembled Polyelectrolyte Microcapsules. *Langmuir* **2010**, *26*, 12575–12584.

43. Hayward, R. C.; Utada, A. S.; Dan, N.; Weitz, D. A. Dewetting Instability During the Formation of Polymersomes from Block-Copolymer-Stabilized Double Emulsions. *Langmuir* **2006**, *22*, 4457–4461.

44. Shum, H. C.; Lee, D.; Yoon, I.; Kodger, T.; Weitz, D. A. Double Emulsion Templated Monodisperse Phospholipid Vesicles. *Langmuir* **2008**, *24*, 7651–7653.

45. Shum, H. C.; Santanach-Carreras, E.; Kim, J.-W.; Ehrlicher, A.; Bibette, J.; Weitz, D. A. Dewetting-Induced Membrane Formation by Adhesion of Amphiphile-Laden Interfaces. *J. Am. Chem. Soc.* **2011**, *133*, 4420–4426.

46. Lee, M. H.; Hribar, K. C.; Brugarolas, T.; Kamat, N. P.; Burdick, J. A.; Lee, D. Harnessing Interfacial Phenomena to Program the Release Properties of Hollow Microcapsules. *Adv. Funct. Mater.* **2012**, *22*, 131–138.

47. Kim, S.; Nam, J.; Kim, J.; Kim, D.; Han, S.; Weitz, D. Formation of Polymersomes with Double Bilayers Templated by Quadruple Emulsions. *Lab Chip* **2013**, *13*, 1351–1356.

48. Robertson, E. J.; Richmond, G. L. Molecular Insights in the Structure and Layered Assembly of Polyelectrolytes at the Oil/Water Interface. *J. Phys. Chem. C* **2014**, *118*, 28331–28343.

49. Choi, J.; Rubner, M. F. Influence of the Degree of Ionization on Weak Polyelectrolyte Multilayer Assembly. *Macromolecules* **2005**, *38*, 116–124.

50. Windbergs, M.; Zhao, Y.; Heyman, J.; Weitz, D. A. Biodegradable Core−Shell Carriers for Simultaneous Encapsulation of Synergistic Actives. *J. Am. Chem. Soc.* **2013**, *135*, 7933–7937.

51. Déjugnat, C.; Sukhorukov, G. B. pH-Responsive Properties of Hollow Polyelectrolyte Microcapsules Templated on Various Cores. *Langmuir* **2004**, *20*, 7265–7269.

52. Mauser, T.; Déjugnat, C.; Sukhorukov, G. B. Reversible pH-Dependent Properties of Multilayer Microcapsules Made of Weak Polyelectrolytes. *Macromol. Rapid Commun.* **2004**, *25*, 1781–1785.

53. Lu, A. H.; Salabas, E. E. L.; Schüth, F. Magnetic Nanoparticles: Synthesis, Protection, Functionalization, and Application. *Angew. Chem., Int. Ed.* **2007**, *46*, 1222–1244.

54. Park, J.; Joo, J.; Kwon, S. G.; Jang, Y.; Hyeon, T. Synthesis of Monodisperse Spherical Nanocrystals. *Angew. Chem., Int. Ed.* **2007**, *46*, 4630–4660.

55. Wu, Y.; Wu, Z.; Lin, X.; He, Q.; Li, J. Autonomous Movement of Controllable Assembled Janus Capsule Motors. *ACS Nano* **2012**, *6*, 10910–10916.

56. Sau, T. K.; Murphy, C. J. Seeded High Yield Synthesis of Short Au Nanorods in Aqueous Solution. *Langmuir* **2004**, *20*, 6414–6420.

57. Charati, M. B.; Lee, I.; Hribar, K. C.; Burdick, J. A. Light-Sensitive Polypeptide Hydrogel and Nanorod Composites. *Small* **2010**, *6*, 1608–1611.

58. Kuo, T.-R.; Hovhannisyan, V. A.; Chao, Y.-C.; Chao, S.-L.; Chiang, S.-J.; Lin, S.-J.; Dong, C.-Y.; Chen, C.-C. Multiple Release Kinetics of Targeted Drug from Gold Nanorod Embedded Polyelectrolyte Conjugates Induced by near-Infrared Laser Irradiation. *J. Am. Chem. Soc.* **2010**, *132*, 14163–14171.

59. You, J.; Shao, R.; Wei, X.; Gupta, S.; Li, C. Near-Infrared Light Triggers Release of Paclitaxel from Biodegradable Microspheres: Photothermal Effect and Enhanced Antitumor Activity. *Small* **2010**, *6*, 1022–1031.

60. Hribar, K. C.; Lee, M. H.; Lee, D.; Burdick, J. A. Enhanced Release of Small Molecules from Near-Infrared Light Responsive Polymer-Nanorod Composites. *ACS Nano* **2011**, *5*, 2948–2956.

61. Nisisako, T.; Ando, T.; Hatsuzawa, T. High-Volume Production of Single and Compound Emulsions in a Microfluidic Parallelization Arrangement Coupled with Coaxial Annular World-to-Chip Interfaces. *Lab Chip* **2012**, *12*, 3426–3435.

62. Romanowsky, M. B.; Abate, A. R.; Rotem, A.; Holtze, C.; Weitz, D. A. High Throughput Production of Single Core Double Emulsions in a Parallelized Microfluidic Device. *Lab Chip* **2012**, *12*, 802–807.

63. Kim, S.-H.; Kim, J. W.; Kim, D.-H.; Han, S.-H.; Weitz, D. A. Enhanced-Throughput Production of Polymersomes Using a Parallelized Capillary Microfluidic Device. *Microfluid. Nanofluid.* **2013**, *14*, 509–514.

64. Tu, F.; Lee, D. Controlling the Stability and Size of Double-Emulsion-Templated Poly (Lactic-Co-Glycolic) Acid Microcapsules. *Langmuir* **2012**, *28*, 9944–9952.